Journal of Nepal Geological Society, 2023, Vol. 65 (Sp. Issue), pp. 1–12
https://doi.org/10.3126/jngs.v65i01.57738

Structure and emplacement of leucogranites along the Manaslu – Himalchuli Himalaya, Nepal

Mike Searle[1,2,3,*] and John Cottle[4]

[1]*Department of Earth Sciences, Oxford University, South Parks Road, Oxford OX1 3AN, UK*
[2]*Oxford University Museum of Natural History, Parks Road, Oxford OX1 3PW*
[3]*Camborne School of Mines, University of Exeter (Cornwall campus), Penryn, Cornwall TR10 9EZ*
[4]*Department of Earth Science, University of California, Santa Barbara, CA USA*
**Corresponding author's email: mike.searle@earth.ox.ac.uk*

ABSTRACT

New field mapping data show that the Manaslu leucogranite (Qtz + Plag + Kfs + Ms + Tur ± Bt ± Grt) in Nepal is a composite intrusion derived from a heterogeneous migmatite melt source at depth, and made up of numerous sills parallel to the main foliation, and dipping shallowly to the north. Crustal thickening led to partial melting and formation of leucogranite melts along the top of the GHS, from earlier muscovite dehydration to later biotite dehydration melting with time. The granite was not a diapiric intrusion and does not intrude across the STD low-angle normal fault. A low-angle, north-dipping normal fault, the ductile-brittle Nar-Phu detachment wraps around the top of the Manaslu leucogranite and truncates all leucogranites in the footwall. The detachment formed the roof fault during exhumation of footwall rocks (channel flow) along the upper GHS during the early-middle Miocene. Metamorphism is also entirely regional and not contact metamorphism. U-Th/Pb monazite ages from metapelites show semi-continuous metamorphism across the GHS from ~35-15 Ma. The leucogranites were emplaced as layer-parallel sills entirely within the GHS between ~25-18.5 Ma. U-Th/Pb monazite dates from the Manaslu leucogranites suggest two major intrusion phases at 22.5 Ma (Larke-la phase) and 19.5 Ma (Bimtang phase). The sheeted sill complex was emplaced by progressive underplating with the oldest intrusions structurally above the younger ones. The migmatite melt source was likely buried further to the north. GHS rocks structurally beneath the Manaslu granite show few leucogranite dykes. Heat for granite melting was entirely internally derived radioactive heating from crustal thickening, and had no frictional heat input from the Main Central Thrust >10-15 km structurally below the base of the leucogranite sheeted sill complex.

Keywords: Manaslu Himalaya, leucogranite, emplacement, South Tibetan Detachment, U-Th/Pb monazite dating

Received: 24 February 2023 **Accepted:** 15 May 2023

INTRODUCTION

The Manaslu pluton forms one of the larger Himalayan leucogranite intrusions in Nepal. It is located along the upper parts of the Greater Himalayan Sequence (GHS) – the metamorphic core of the Himalaya, bounded by the South Tibetan Detachment STD) low-angle normal fault along the top and the Main Central Thrust (MCT) ductile shear zone along the base (Fig. 1). Early mapping suggested that the Manaslu leucogranite was a pluton with a contact metamorphic aureole around the margin, and intruded across the STD into the Tethyan sedimentary sequence (TSS) above (Colchen et al., 1986; LeFort, 1975, 1981; Guillot et al., 1993, 1995). Later regional mapping showed that the Manaslu leucogranite was entirely within the GHS and structurally below a major regional low-angle ductile shear zone – normal fault, the Nar-Phu detachment, which wraps around the upper margin of the leucogranite (Searle and Godin, 2003; Searle, 2010). These authors also showed that the GHS metamorphism was entirely regional Barrovian-type, and not contact metamorphism at all. Indeed, the leucogranites were intruded into sillimanite-grade gneisses and migmatites which now underlie the Manaslu leucogranite. The detailed internal structure of the Manaslu leucogranite remains poorly known, partly because of the extreme steepness and inaccessibility of the terrain.

The earliest melting events in the Annapurna-Manaslu Himalaya are recorded in low-volume kyanite-bearing leucosomes formed at PT conditions of 720-710ºC and 1.1-1.0 kbar during the time span 25-18 Ma (Iaccarino et al., 2015). Most large-scale melting along the Himalaya is related to muscovite or biotite dehydration and occurred during the period 25-19 Ma, although younger leucogranites have been dated as young as 15.4 Ma in the Rongbuk valley (Cottle et al., 2015). The two melting reactions relevant are the muscovite melting reaction (Eq. 1, 2):

$$Ms + Pl + Qtz \pm Grt = Kfs + Sil + Bt + Liquid\ (melt) \quad (1)$$

and the biotite dehydration reaction.

$$Bt + Pl + Qtz + Sil = Grt + Kfs + Liquid\ (melt) \quad (2)$$

At pressures <5 kbar cordierite may form as a magmatic phase, whereas garnet is the stable phase at pressures >5 kbar. Tourmaline is present in varying amounts throughout

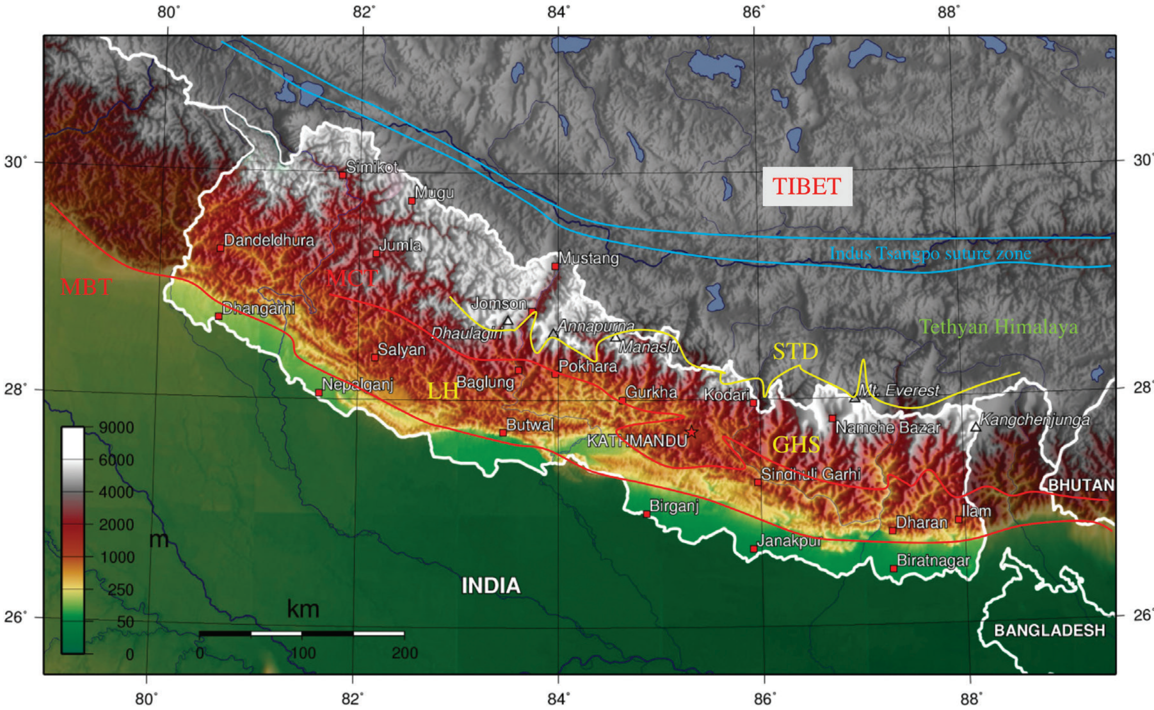

Fig. 1: Digital Elevation map of Nepal Himalaya showing the major geological zones across the Himalaya. STD – South Tibetan Detachment; MCT – Main Central Thrust; MBT – Main Boundary Thrust.

Himalayan leucogranites and reflects high boron concentrations in the protolith sedimentary rocks. Some leucogranites have magmatic andalusite (Visona et al., 2012) and several, including the large Makalu leucogranite, have magmatic cordierite (Streule et al., 2010; Searle et al., 2010). The leucogranites are entirely crustal melts (Harris and Massey, 1994; Harris et al., 2000) and are likely derived from melting a shale-psammite protolith, such as the Proterozoic Haimanta shales (Searle et al., 2010).

Few studies have mapped out the Himalayan leucogranites in detail, leading to controversies regarding their isotopic heterogeneity, the migmatite source regions, their emplacement mechanisms and their internal structure. Mapping of the Everest – Nuptse leucogranites has revealed that the leucogranites were intruded as large-scale sills intruding the high-grade gneisses along the top of the GHS (Searle, 1999a,b). These sills sometimes ballooned outwards to form bulbous structures, as seen in the Nuptse leucogranite (Searle et al., 2003, 2006). Outlier peaks of Everest, such as Ama Dablam, show thick leucogranite sills dipping at low angle to the north, with narrow dykes feeding magma into overlying sills (Searle et al., 2003, 2010). These dykes at the highest structural level are rotated towards the north showing that the motion along the STD was southward extrusion of footwall. These combination of filed structural mapping, thermobarometry, strain analyses and U-Th/Pb geochronology led to the Channel flow model, where a mid-crustal layer of high-grade metamorphic rocks, migmatites and leucogranites were extruded to the south, bounded by high-strain ductile shear zones above (STD) and below (MCT) (Searle and Rex, 1989; Searle et al., 2003, 2006, 2008, 2010; Grujic et al., 2002; Grujic, 2006; Law et al., 2004, 2011; Searle and Szulc, 2005; Jessup et al., 2006, 2008; Cottle et al., 2007, 2009, 2015).

This paper describes the field relationships within and around the Manaslu - Himalchuli leucogranite in detail (Fig. 2). We propose a model for leucogranite generation and emplacement based on field relationships, themobarometric data, and extensive U-Th/Pb monazite dating, as summarised in Cottle et al. (2019). We also compare the structure of the Manaslu-Himalchuli leucogranite to that of the Everest-Lhotse, Makalu, and Kanchenjunga-Jannu leucogranites in Nepal.

REGIONAL GEOLOGY AROUND THE MANASLU - HIMALCHULI RANGE

The internal structural units of the GHS were initially described as Formation I (dominantly pelites), Formation II (dominantly calc-silicates and hornblende-biotite schists) and Formation III (dominantly augen gneisses) (Bordet et al., 1975; LeFort, 1975; Colchen et al., 1986). These metamorphic rocks were reassigned as Units rather than sedimentary formations by Searle and Godin (2003). The Chame detachment was described as a ductile shear zone with mylonite fabrics placing Tibetan meta-sedimentary rocks above high-grade metamorphic rocks of the GHS below (Coleman, 1996, 1998). Gleeson and Godin (2006) and Searle (2010) recognised two additional GHS units structurally above the Chame detachment, Unit IV composed of 500 m thick dominantly phlogopite-bearing marbles, and Unit V composed of 500 m thick garnet + biotite phyllite and schist (Fig. 3). The entire GHS has been folded by large-scale open folds recognised from the Mutsog synform in the lower Marysandi valley and the Chako antiform in the upper Nar-Phu valley (Fig. 2). Searle and Godin (2003) mapped a major zone of ductile strain approximately 350 m thick, overprinted by later brittle structures, termed the Phu detachment which separates metamorphic rocks below (biotite + phlogopite marbles, diopside + K-feldspar calc-silicates, and leucogranite

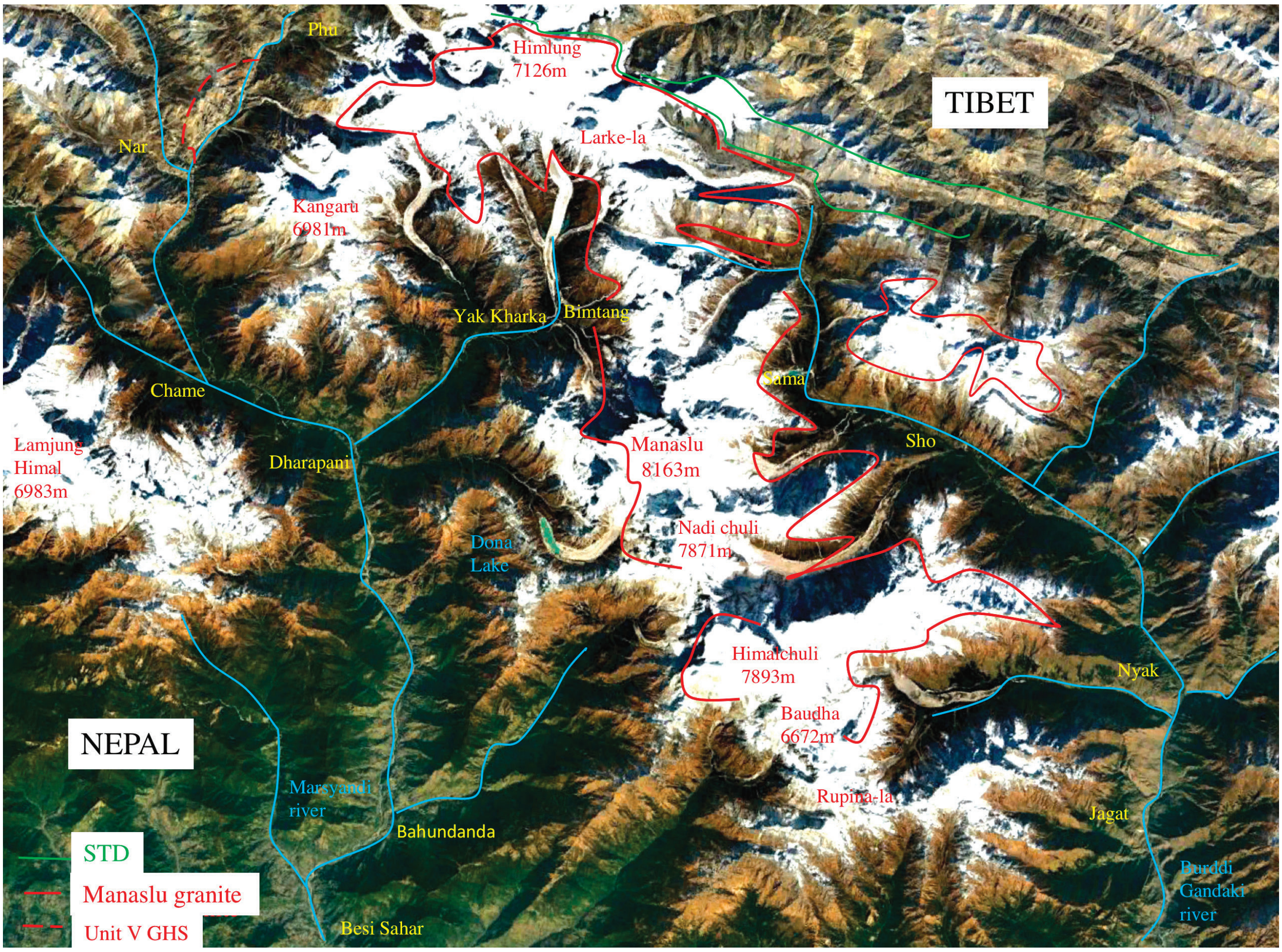

Fig. 2: Google Earth image of the Manaslu–Himalchuli Himalaya in Nepal, showing the approximate outline (red) of the Manaslu leucogranite, and the Phu Detachment (South Tibetan Detachment).

dykes and sills) from unmetamorphosed sedimentary rocks above. The Phu detachment wraps around the Chako dome and also along the upper contact of the Manaslu leucogranite. The leucogranite is therefore entirely within the GHS, and does not intrude across the low-angle normal fault into the overlying sedimentary rocks (Fig. 3). The Phu detachement correlates westward to link with the Machapuchare detachment in the Annapurna Sanctuary region (Fig. 4) (Searle, 2010). These low-angle normal faults both place unmetamorphosed sedimentary rocks above metamorphic rocks and are regarded as the true STD. The structurally lower Chame detachment separates Units II and III below from Units IV and V above (Gleeson and Godin, 2006).

Several structural discontinuities have been proposed within the GHS in Nepal, some clearly thrust-related, such as the Khumbu thrust in the Everest region (Searle, 1999; Searle et al., 2003, 2006), and thrusts in the Kangchengjunga region (Ambrose et al., 2015), others extension-related (Hodges et al., 1996; Goscombe et al., 2006; Searle, 2010; Larson and Cottle, 2014; Montomoli et al., 2013). These detachments however are not entirely compressional or extensional in origin. Most have a history that includes early south-directed simple shear thrust fabrics overprinted by later top-north 'extensional' fabrics. This is consistent with the metamorphic evidence that shows the prograde burial history was followed by later retrograde exhumation 'normal sense' fabrics imposed as rocks were transferred from footwall burial to hanging-wall exhumation with time. These extensional fabrics do not relate to any crustal or lithospheric extension, but instead relate to extrusion of the footwall during active compression (Searle, 2010, 2013).

The most contentious structure within the GHS is the so-called High Himalayan Thrust (HHT) proposed by Goscombe et al. (2006, 2018). This cryptic structure has been inferred from tectono-metamorphic breaks in PT conditions, lithological difference and/or differences in geochronology across the structure (Groppo et al., 2009; Montomoli et al., 2013). The HHT corresponds to a metamorphic isograd, either the kyanite-sillimanite isograd, or the sillimanite + K-feldspar + melt isograd, where abundant migmatites occur above compared to few below. There is no exceptional high strain zone associated with this contact given that crustal melting has often obliterated earlier structures and fabrics. The main question therefore is: Is the HHT a metamorphic boundary, or is it a ductile shear zone, or both?

THE MANASLU – HIMALCHULI LEUCOGRANITE

The map outline of the Manaslu leucogranite is shown in Figure 2. It covers the upper levels of Manaslu (8163 m), Nadi chuli (7871 m), and Himalchuli (7893 m), extending SE towards the

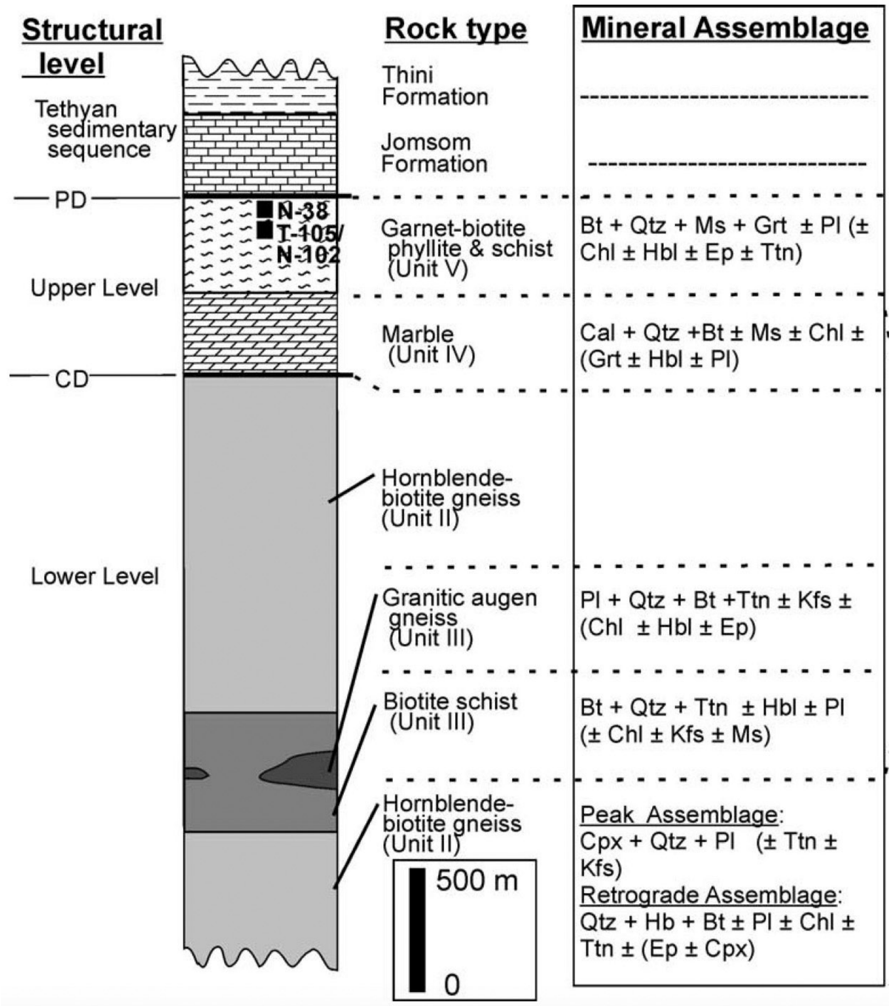

Fig. 3: Log section showing lithology and mineral assemblages of Units II – V of the Greater Himalayan Sequence in the Manaslu and Annapurna Himalaya (after Searle and Godin, 2003; Gleeson and Godin, 2006).

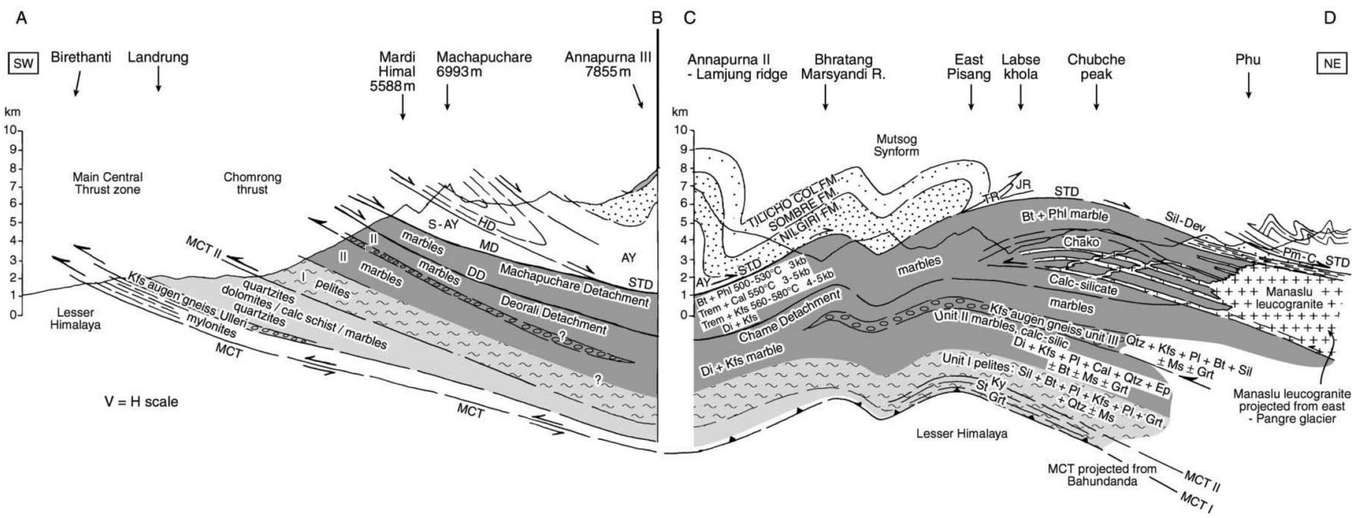

Fig. 4: Composite cross-section of the Annapurna – Manaslu Himalaya, after Searle and Godin (2003) showing the structural position of the Manaslu leucogranite and Chako dome within the Greater Himalayan Sequence.

peak of Baudha (6672 m). To the NW, the leucogranite cuts across the Larke-la pass to the peaks of Himlung (7126 m) and Cheo (6812 m). The Manaslu leucogranite is a peraluminous, alkali-rich minimum melt granite composed of the assemblage: Qtz + Pl + Kfs + Tur + Ms ± Bt ± Grt. The leucogranites are heterogeneous and show a variety of mineralogy and texture, including tourmaline + garnet leucogranite (Fig. 5a), two-mica leucogranites (Fig. 5b). Migmatite leucosomes contain sillimanite clusters (Fig. 5c) and can be seen to have *in situ* melting textures (Fig. 5d). The Manaslu leucogranite has variable amounts of tourmaline as a primary magmatic phase. High initial $^{87}Sr/^{86}Sr$ ratios (0.74–0.78) high concentrations of U, Th and other heat-producing elements suggest it was entirely derived from melting of continental crustal rocks with no input from the mantle (LeFort, 1981; Vidal et al., 1982).

The north face of Manaslu shows spectacular cliffs over 4,500 meters high with layered leucogranites dipping to the north, overlying a melt zone where leucogranite has broken up xenoliths of GHS pelitic gneiss protolith (Fig. 6a). The internal structure of the Manaslu leucogranite shows a series of

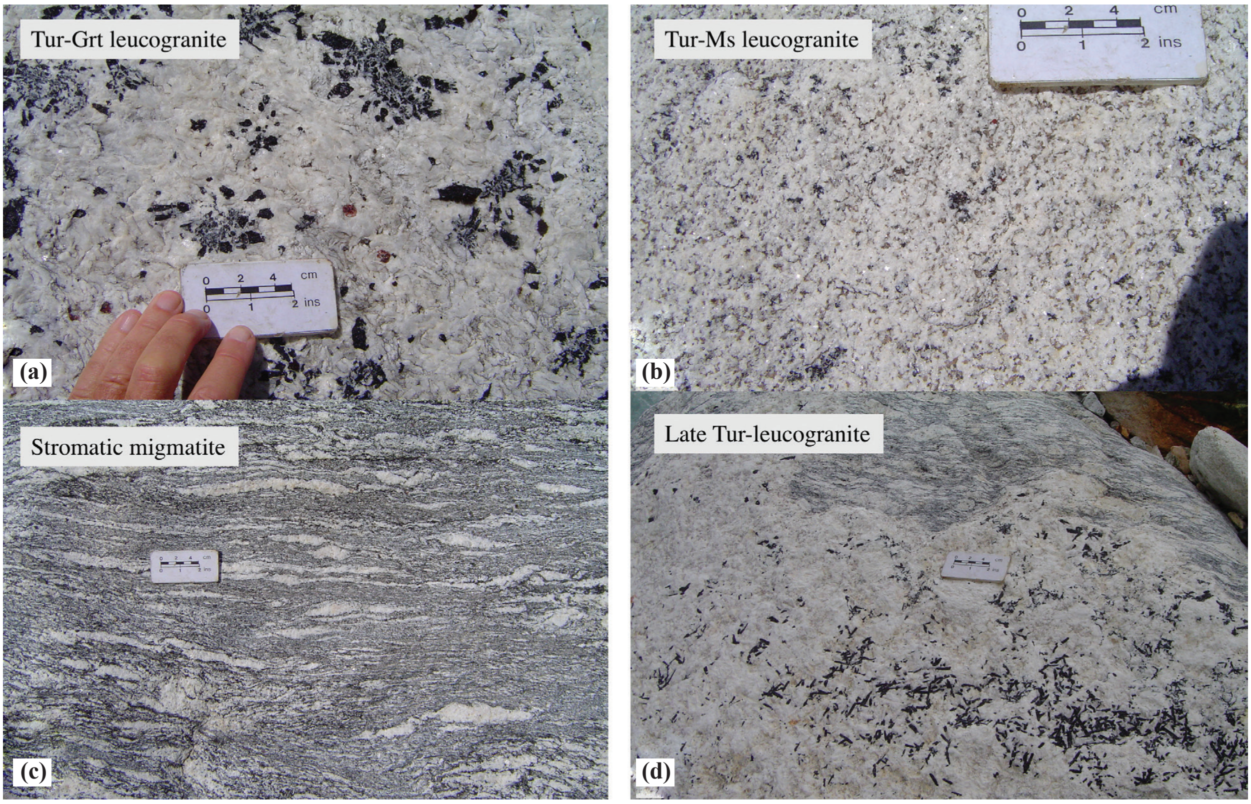

Fig. 5: Main granite lithologies of the Manaslu Himalaya (a) Tourmaline + garnet leucogranite, (b) two-mica leucogranite with minor tourmaline, (c) stromatic migmatite showing *in situ* melting with leucosome streaks parallel to the main schistosity, (d) late-stage Tourmaline + garnet + muscovite leucogranite cutting earlier migmatite schistosity.

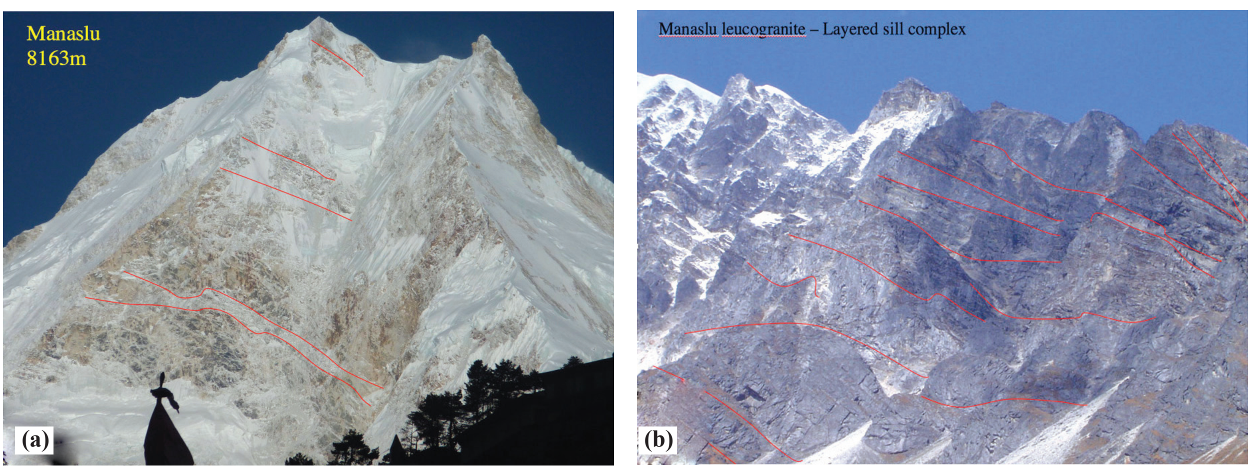

Fig. 6: (a) The NE face of Manaslu from Sho village, showing 4500 m high cliffs of layered leucogranites dipping at low angle to the north, (b) central part of the Manaslu leucogranite showing layered sheeted sill complex with at least 7 foliation-parallel sills that make up the pluton.

between 12–17 parallel sills intruded as a sheeted sill complex, dipping at low angle to the north (Fig. 6b). Occasional schlieren of black sillimanite gneisses sometimes separate these leucogranite sills, whereas in other places sills are intruded into earlier leucogranites by underplating, and magma injection along schistosity planes. The uppermost leucogranite sill is exposed above the Larke-la (Fig. 7a) where a shear zone separates the leucogranite below from the overlying Tethyan zone sedimentary rocks. Massive leucogranites up to 4 km thick form the cliffs above Bimtang along the western margin of the Manaslu leucogranite (Fig. 7b). The roof of the leucogranite is exposed along the summit ridge at 8200 meters altitude. The melt source region lies to the north beneath the Tethyan zone but there are outcrops around Bimtang where *in situ* stromatic migmatites showing the earliest melt veins have been intruded by at least two sets of cross-cutting leucogranite dykes (Fig. 8a,b). These late cross-cutting dykes have variable amounts of tourmaline, and occasional schorl tourmaline + quartz vugs. The upper levels of Manaslu and Himalchuli are extremely difficult to access, but both mountains show leucogranite cliffs extending up to the summit, and leucogranite sheets dipping gently towards the north or NNE (Fig. 9a). The base of the north face of Manaslu shows a spectacular zone of in situ melting where white leucogranite has intruded and broken up xenoliths of dark-coloured GHS country rocks (Fig. 9b).

The Chako dome west of the main Manaslu leucogranite, shows the uppermost levels of the GHS structurally immediately beneath the lower Manaslu leucogranite sheets (Fig. 10a). Here, garnet biotite schists, calc-silicates and marbles have been intruded by at least two sets of leucogranites, similar to the migmatite-granite outcrops near Bimtang. Early leucogranite sills are parallel to the metamorphic foliation and the *in situ* leucosomes in the sillimanite gneisses. Later, more leucocratic tourmaline leucogranite dykes cross-cut the metamorphic fabrics and early stromatic migmatite fabrics (Fig. 10b).

GEOCHRONOLOGY OF THE MANASLU PLUTON

Numerous studies have reported isotopic ages for the Manaslu pluton. The earliest studies employed the Rb/Sr technique with limited success, largely due to extreme initial $^{87}Sr/^{86}Sr$ isotopic heterogeneities that make calculating precise ages difficult. Nevertheless, such studies confirmed a Miocene age for the pluton (Hamet and Allègre, 1978, 1976; Vidal, 1978; Vidal et al., 1982; Deniel et al., 1987). Subsequent studies have largely employed U-Th/Pb accessory phase geochronology, and despite complexities from Pb-loss, inheritance, and/or protracted crystallization, have outlined, in detail, the emplacement history of the pluton. These data suggest emplacement of the Manaslu pluton was dominated by

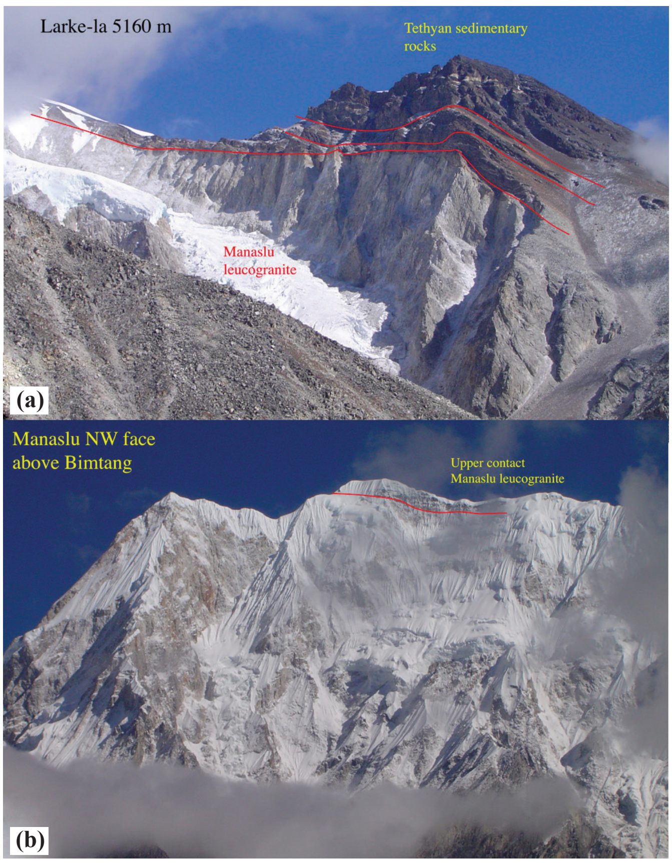

Fig. 7: (a) The upper contact of the Manaslu leucogranite north of the Larke-la (5160 m). The Phu detachment shows a high strain zone separating leucogranites below from unmetamorphosed Tethyan sedimentary rocks above, (b) four kilometre high cliffs of Manaslu leucogranite above Bimtang with the upper contact visible along the summit ridge.

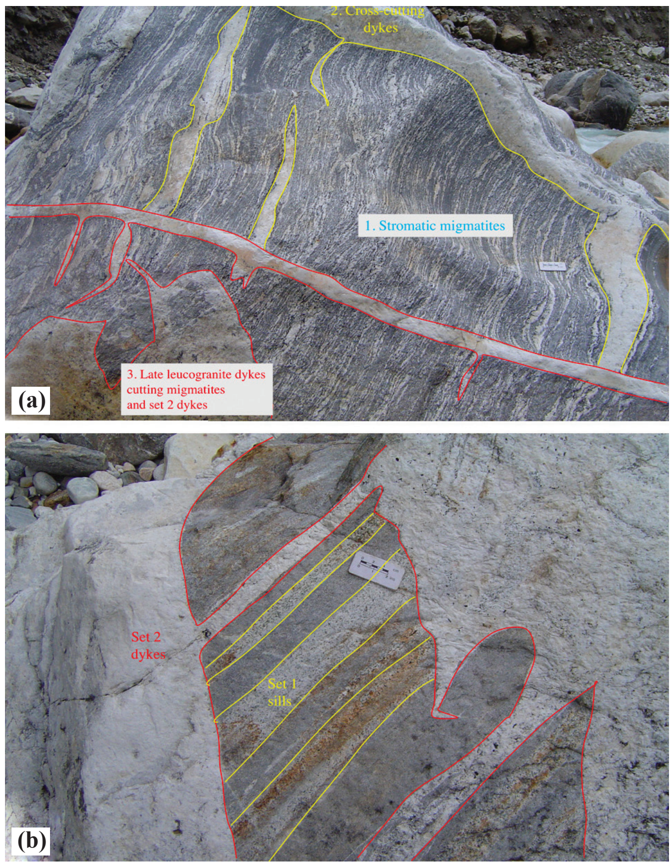

Fig. 8: (a, b) Outcrops above Bimtang showing structural relations of the lower melting zone of the Manaslu leucogranite. In situ migmatites show early foliation-parallel sills (yellow) cut by later more leucocratic tourmaline granites (red).

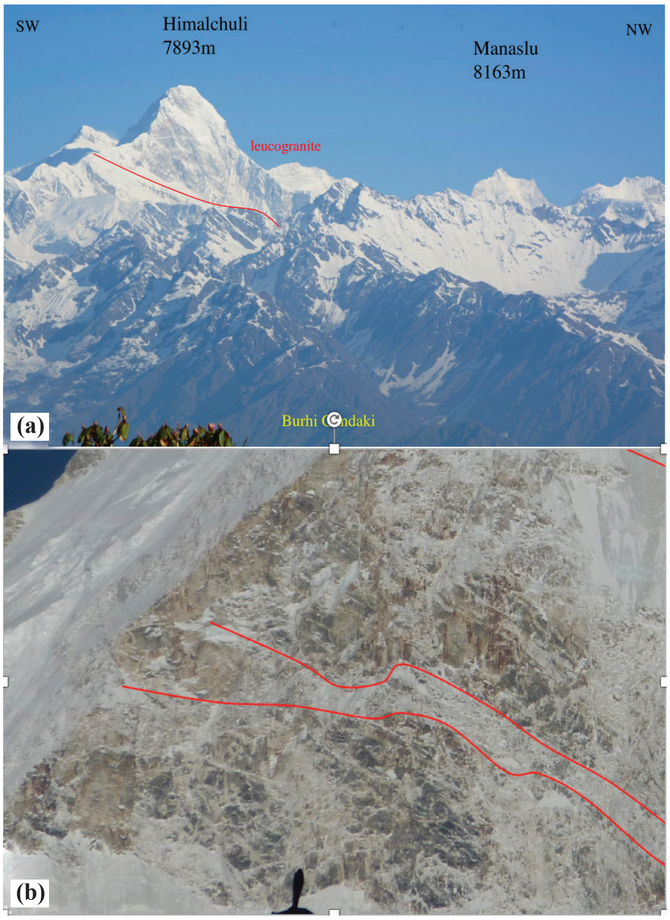

Fig. 9: (a) The Himalchuli and Manaslu massifs viewed from the Ganesh Himal across the Buddhi Gandaki river, above Kashigaon-Yarsa villages, showing the north-dipping leucogranite sheet above the banded GHS gneisses, (b) close-up of the melting zone of the Manaslu leucogranite in cliffs along the base of the NE face.

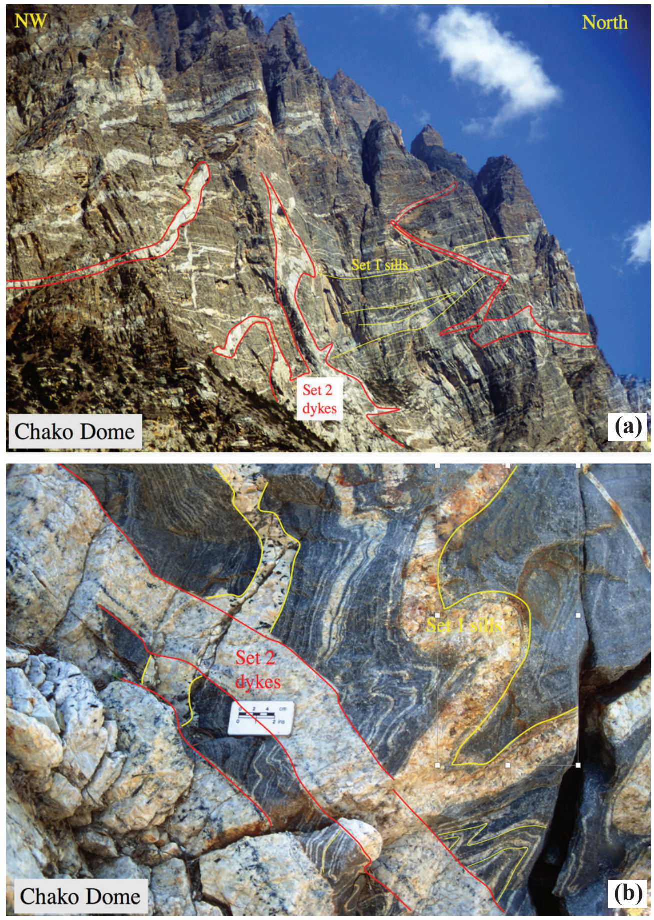

Fig. 10: (a) The Chako dome along the Nar – Phu valley west of Himlung and the main Manaslu leucogranite. These are garnet-biotite gneisses, calc-silicates and marbles intruded by leucogranite sills (yellow) cut by later cross-cutting leucogranite dykes (red), (b) outcrop of the Chako dome showing early foliation-parallel sills (yellow) cut by later leucocratic dykes.

two pulses – the Larkya La phase c. 22 Ma, and the younger, c. 19 Ma, Bimtang phase (Harrison et al., 1995, 1999). A subsequent, larger-scale, monazite study recognized the same two age peaks, argued that the older Larkya La phase maybe be as old as c. 25 Ma, and recognized subordinate peaks at ~21.4 Ma and ~16 Ma (Fig. 11; Cottle et al., 2019).

Concomitantly with the monazite isotopic dates, Cottle et al. (2019) collected in-situ Sm/Nd isotopes and trace element concentrations. Combined, these results indicate that the structurally higher portions of the pluton are generally older, and have less negative εNdi values, less inheritance, lower Y, and higher Gd/Yb compared to structurally lower samples. These systematic age and geochemical trends led Cottle et al. (2019) to infer that the Manaslu pluton was constructed from the top downward, with successive phases of melt emplaced at lower structural positions, and that melt was progressively extracted from an increasingly REE-fractionated source region(s) in the presence of lower proportions of water and at lower temperatures. In addition, the Sm/Nd data indicate that monazite dissolution and melt homogenization was less efficient in structurally lower rocks, implying a change in the melt-forming reaction and/or prolonged phosphorous saturation as a function of time.

DISCUSSION

Detailed mapping around the Manaslu leucogranite reveals that the intrusion is composed of a series of >20 foliation-parallel sills emplaced from the north. The *in situ* melt generation zone may be exposed along the lower cliffs above Sho and Sama villages along the northern margin of the leucogranite. The upper contact of the leucogranite is well exposed along the high mountains north of the Larke-la, and dips at only 10º to the north. The summit of Manaslu shows leucogranite intrusions into black gneisses also seen along the top of the Bimtang cliffs (Manaslu north). U-Th/Pb age data suggest construction of the leucogranite from the top down. This suggests downward migration of isotherms during unroofing of the GHS by the STDS (Phu and Chame detachments; Searle and Godin, 2003; Godin et al., 2006; Gleeson and Godin, 2006; Cottle et al., 2015, 2019). The Chako dome, west of the main Manaslu leucogranite also shows several sets of leucogranites intruding high-grade gneisses and marble of the uppermost GHS. The

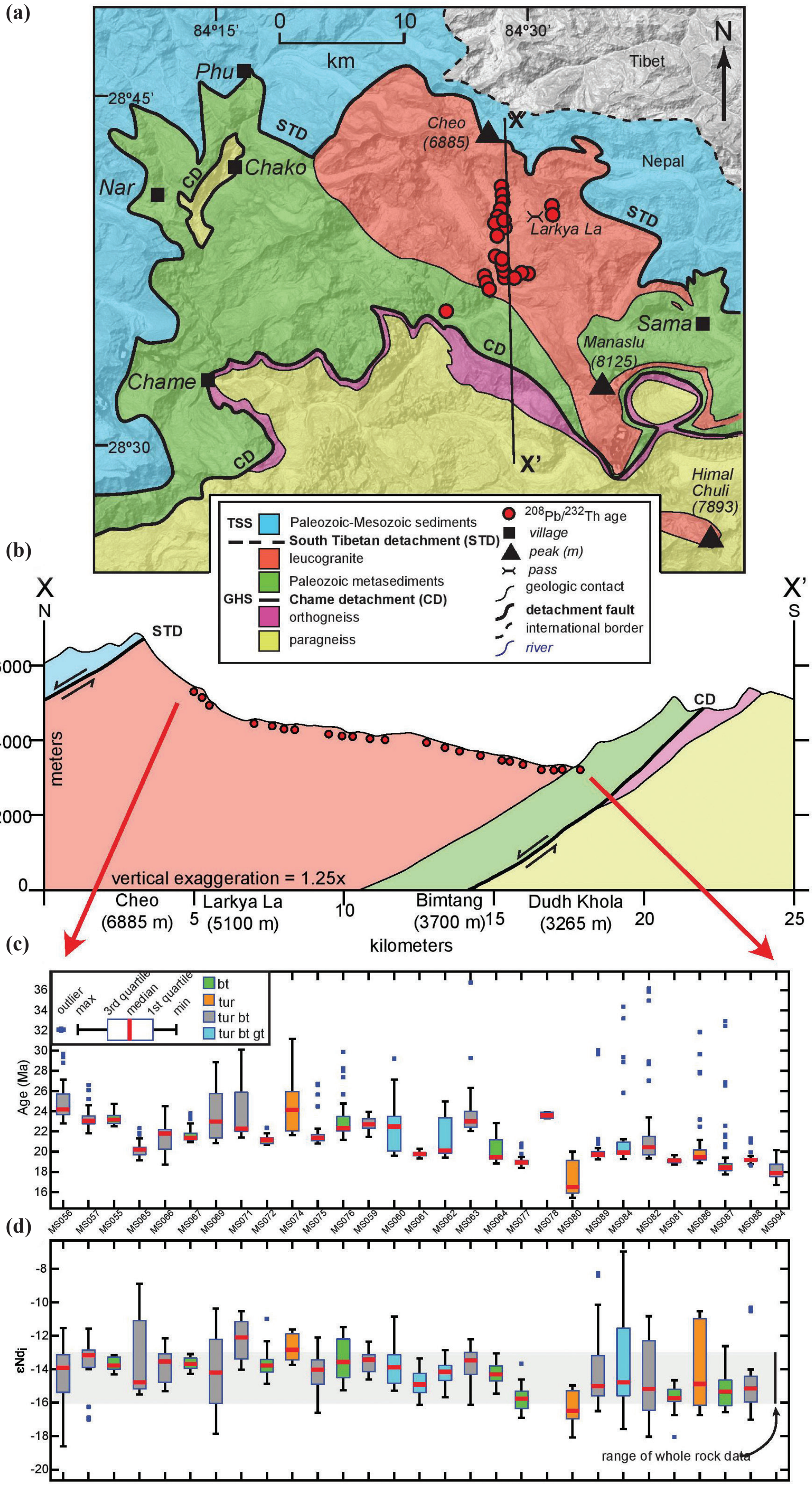

Fig. 11: Geologic map (a) and cross section, (b) of the Manaslu region with sample locations, from Cottle et al. (2019). GHS, Greater Himalayan Sequence; TSS, Tibetan sedimentary series, (c) 208Pb/232Th date and, (d) monazite εNd box and whisker plots illustrating values contained in each sample relative to their structural position. The range of whole rock Nd for Manaslu pluton is compiled from Deniel et al. (1987), Stern et al. (1989), and Harrison et al. (1999) (modified after Cottle et al., 2019).

cliffs along the southern margin of Manaslu above Dona Lake show well layered gneisses with very few leucogranite dykes. Nowhere does the Manaslu leucogranite intrude across the STD low-angle normal fault.

The structural geometry of the Manaslu – Himalchuli leucogranite is very similar to the structure of other large Himalayan leucogranites such as Shisha Pangma (Searle et al., 1997), Everest – Nuptse (Searle, 1999a,b; Searle et al., 2003, 2006), Makalu (Streule et al., 2010), and Kangchenjunga – Jannu (Searle and Szulc, 2005). All these leucogranites show an internal structure dominated by large foliation-parallel sills, a migmatitic melt zone, a structural position beneath the north-dipping STD low-angle normal fault, and a location along the top of the GHS. Similar timing of shearing along the STD ductile shear zone and normal fault, and the MCT ductile shear zone and normal fault supports the model of Channel flow, the ductile extrusion towards the south of a mid-crust partially molten slab. The structure of the Manaslu – Himalchuli Himalaya might suggest that the base of the ductile channel occurred along the base of the leucogranite, rather than along the MCT zone. Wherever one draws the base of the ductile channel the GHS structures are almost entirely ductile and show simple shear top-to-south fabrics, combined with a significant proportion of pure shear (Law et al., 2004, 2011; Parsons et al., 2016a,b). Along the upper part of the GHS, fabrics are mainly overprinted by top-to-north ‘extensional’ fabrics. These fabrics record southward thrusting and extrusion of the footwall rocks and not any regional extension (Searle, 2010, 2013).

Beneath the Manaslu leucogranite the GHS shows a 30–35 km thick thrust sheet of metamorphic rocks (Godin et al., 2001; Larson et al., 2011; Parsons et al., 2016a,b,c). These are mainly Proterozoic to Cambrian-Ordovician protoliths that were metamorphosed during late Eocene to Miocene time. Older Paleoproterozoic protoliths occur along the Lesser Himalaya south of the MCT and also along the northern part of the GHS (Ama Drime massif, Nanga Parbat). Numerous authors have previously defined the MCT on spurious criteria (lithological differences, detrital zircon ages, Nd isotope signatures, metamorphic isograds), none of which can be used to define a thrust fault or ductile shear zone. Searle and Rex (1989), Grujic et al. (1996, 2002), Stephenson et al. (2001), Searle et al. (2003, 2006, 2008) Law et al. (2004, 2011), Godin et al. (2006), Larson et al. (2011) and Parsons et al. (2016a,b,c) defined the MCT on strain criteria. These authors all placed the MCT along the base of the inverted metamorphic sequence (MCT zone) and not along the kyanite isograd (Colchen et al. 1986; Kohn, 2008; Martin et al., 2005, 2010; Catlos et al., 2001, 2018; Shrestha et al., 2020).

CONCLUSIONS

- The Manaslu leucogranite is a large composite leucogranite intrusion made up of >20 foliation-parallel sills that were intruded into sillimanite-bearing gneisses, calc-silicates and marbles along the top of the GHS.
- The Manaslu leucogranite was not emplaced as a diapiric pluton, and does not cross-cut the STD low-angle normal fault, or intrude into the Tethyan sedimentary sequence (Colchen et al., 1986; LeFort, 1981; Guillot et al., 1993). The Nar-Phu detachment, part of the STD low-angle normal fault system, wraps around the top of the Manaslu leucogranite (Searle and Godin, 2003; Searle, 2010).
- U-Th/Pb monazite ages suggest that Manaslu leucogranite sills were emplaced from the top downwards, over a period of ~3 m.y. from ~22.5 Ma (Larke-la phase) to ~19.5 Ma (Bimthang phase) (Cottle et al., 2019).
- The leucogranites formed entirely by crustal melting with no mantle input. Source rocks were dominantly boron-rich shales-pelites and psammites of Neoproterozoic age, although elsewhere along the Himalaya, some leucogranites show an increasingly older Paleoproterozic source region (Hopkinson et al., 2020).
- The melt source region shows isotopic heterogeneity (^{143}Nd/^{144}Nd and Sm-Nd isotopes; Cottle et al., 2019) and is likely buried at depth to the north. Some outcrops along the base of the north face of Manaslu may show the actual *in situ* melt zone.
- Metamorphic rocks of the GHS structurally beneath the Manaslu leucogranite show clockwise PTt paths and monazite growth over the period at least 43 Ma to 15 Ma (Larson et al., 2011). The first crustal melts are small volume kyanite-bearing leucosomes (~710ºC, 1.1 GPa; Iaccarino et al., 2015), formed at greater depth and more common in the Annapurna massif to the west. They were followed by more widespread muscovite dehydration melting, decompression-related, sillimanite-bearing melts, formed at lower pressure (~650ºC; 0.7 GPa). The Manaslu - Himalchuli leucogranites were formed by the latter melt reaction.
- GHS rocks beneath the Manaslu leucogranite show a southward propagating structural evolution where footwall rocks show a burial prograde evolution at the same time as hangingwall rocks show a retrograde cooling during exhumation. Likewise, top-south compressional fabrics are overprinted by top-north (actually footwall to south) fabrics as rocks were progressively exhumed.
- The High Himalayan Discontinuity (Goscombe et al., 2018) is dominantly a metamorphic boundary, not a structural one, representing the sill + Kfs + melt-in reaction, and the appearance of abundant migmatite melts above.
- Channel Flow models and thrust wedge (critical taper) models are not mutually exclusive (Kohn, 2008; He et al., 2015). Most of the GHS rocks show ductile fabrics which evolve to brittle thrust-related fabrics with time and exhumation (decreasing P and T).
- The Main Central Thrust outcrops ~50 km south of the Manaslu leucogranite and follows the base of the inverted metamorphic sequence (Searle et al., 2008), not the kyanite-in isograd (Colchen et al., 1986; Kohn, 2008; Martin et al., 2010; Shrestha et al., 2020). A general pattern of progressively younger metamorphic monazite ages (20-6 Ma) towards the south characterises the MCT ductile shear zone (Catlos et al., 2001, 2018). These ages record the south-directed in-sequence accretion of footwall slices over the Miocene.

- Any frictional heating generated along the MCT played no role in the generation of the Himalayan leucogranites some 15–20 km structurally up-section.

ACKNOWLEDGEMENTS

Mike Searle thanks the Leverhulme Trust for funds enabling fieldwork in Nepal. John Cottle was supported by a US National Science Foundation grant (EAR-1119380).

REFERENCES

Ambrose, T. K., Larson, K. P., Guilmette, C., Cottle, J. M., Buckingham, J. M., and Rai, S., 2015, Lateral extrusion, underplating, and out-of-sequence thrusting within the metamorphic core, Kangchenjunga, Nepal. Lithosphere, L437-1.

Bordet, P., Colchen, M., Krummenacher, D., LeFort, P., Mouterde, R., and Remy, M. 1971, Recherche géologiques dans l'Himalaya du Népal: région de la Thakkhola. CNRS, Paris, 279 p.

Catlos, E. J., Harrison, T. M., Kohn, M. J., Grove, M., Ryerson, F. J., Manning, C. E., and Upreti, B. N., 2001, Geochronologic and thermobarometric constraints on the evolution of the Main Central thrust, central Nepal Himalaya. Jour. Geophys. Res., v. 196, pp. 16177–16204.

Catlos, E. J., Harrison, T. M., Manning, C. E., Grove, M., Rai, S. M., Hubbard, M., and Upreti, B. N., 2002, Records of the evolution of the Himalayan orogen from in situ Th-Pb ion microprobe dating of monazite: Eastern Nepal and western Garhwal. Journal of Asian Earth Sciences, v. 20, pp. 459–79.

Colchen, M., LeFort, P., and Pêcher, A., 1986, Annapurna – Manaslu – Ganesh Himal, CNRS, Paris, 136 p.

Coleman, M. E., 1996, Orogen-parallel and orogen perpendicular extension in the central Nepal Himalaya. Geol. Soc. Am. Bull., v. 108, pp. 1594–1607.

Coleman, M. E., 1998, U-Pb constraints on Oligocene – Miocene deformation and anatexis within the central Himalaya, Marsyandi valley, Nepal. Am. Jour. Sci., v. 298, pp. 553–71.

Cottle, J. M., Jessup, M. J., Newell, D. L., Searle, M. P., Law, R. D., and Hortswood, M. S. A., 2007, Structural insights into the early stages of exhumation along an orogeny-scale detachment: the South Tibetan Detachment system, Dzakaa chu section, eastern Himalaya. Jour. Structural Geol., v. 29, pp. 1781–1797.

Cottle, J. M., Searle, M. P., Horstwood, M. S. A., and Waters, D. J., 2009, Timing of mid-crustal metamorphism, melting, and deformation in the Mount Everest region, South Tibet revealed by U(Th)-Pb geochronology. Jour. Geology, v. 117, pp. 643–664.

Cottle, J. M., Larson, K. P., and Kellett, D. A., 2015, How does the mid-crust accommodate deformation in large, hot collisional orogens? A review of recent research in the Himalaya. Jour. Structural Geol., v. 78, pp. 119–133.

Cottle, J. M., Lederer, G., and Larson, K., 2019, The monazite record of pluton assembly: Mapping Manaslu using petrochronology. Chemical Geol., v. 530, p. 119309.

Deniel, C., Vidal, P., Fernandez, A., and LeFort, P., 1987, Isotopic study of the Manaslu granite (Himalaya, Nepal): inferences on the age and source of Himalayan leucogranites. Contr. Min. Pet., v. 96, p. 78–82.

Gleeson, T. P. and Godin, L., 2006, The Chako antiform: A folded segment of the Greater Himalayan sequence, Nar valley, Central Nepal Himalaya. Jour. Asian E. Sci., v. 27, pp. 717–734.

Godin, L., Parrish, R. R., Brown, R. L., and Hodges, K. V., 2001, Crustal thickening leading to exhumation of the Himalayan core of central Nepal: Insight from U-Pb geochronology and $^{40}Ar/^{39}Ar$ thermochronology. Tectonics, v. 20, pp. 729–47.

Godin, L., Grujic, D., Law, R. D., and Searle, M. P., 2006, Channel Flow, Ductile extrusion and exhumation in continental collision zones: an introduction. In: Law, R. D., Searle, M. P., and Godin, L. (eds.), Channel Flow, Ductile extrusion and exhumation in continental collision zones, Geol. Soc. London Spec. Pub., v. 268, pp. 1–23.

Goscombe, B., Gray, D., and Hand, M., 2006, Crustal architecture of the Himalayan metamorphic front in eastern Nepal. Gondwana Res, v. 10(3-4), pp. 232–255.

Goscombe, B., Gray, D., and Foster, D. A., 2018, Metamorphic response to collision in the Central Himalayan orogen. Gondwana Res., v. 57, pp. 191–265.

Groppo, C., Rolfo, F., and Lombardo, B., 2009, P-T evolution across the Main Central thrust zone(Eastern Nepal): hidden discontinuities revealed by petrology. Jour. Petrol., v. 50, pp. 1149–1180.

Grujic, D., 2006, Channel Flow and continental collision tectonics: an overview. In: Law, R. D., Searle, M. P., and Godin, L. (eds.), Channel Flow, Ductile extrusion and exhumation in continental collision zones, Geol. Soc. London Spec. Pub., v. 268, pp. 25–37.

Grujic, D., Casey, M., Davidson, C., Hollister, L., Kundig, K., Pavlis, T., and Schmid, S., 1996, Ductile extrusion of the Higher Himalayan crystalline in Bhutan: evidence from quartz microfabrics. Tectonophys., v. 260, pp. 21–43.

Grujic, D., Hollister, L., and Parrish, R. R., 2002, Himalayan metamorphic sequence as an orogenic channel: insight from Bhutan. Earth and Planetary Science Letters, v. 198, pp. 177–191.

Guillot, S., Pêcher, A., Rochette, P., and LeFort, P., 1993, The emplacement of the Manaslu granite of central Nepal: field and magnetic susceptibility constraints. In: Treloar, P. J. and Searle, M. P. (eds.), Himalayan Tectonics. Geol. Soc. London Spec. Pub., v. 74, pp. 413–428.

Guillot, S., LeFort, P., Pêcher, A., Barman, M. R., and Aprahamian, J., 1995, Contact metamorphism and depth of emplacement of the Manaslu granite (central Nepal). Implications for Himalayan orogenesis. Tectonophys., v. 241, pp. 99–119.

Hamet, J. and Allegre, C. J., 1978, Rb-Sr systematics in granite from Central Nepal (Manaslu): significance of the Oligocene age and high 87Sr/86Sr ratio in Himalayan orogeny. Geology, v. 4, pp. 470–472.

Harris, N. and Massey, J., 1994, Decompression and anatexis of Himalayan metapelites. Tectonics, v. 13, pp. 1537–1546.

Harris, N., Ayres, M., and Massey, J., 1995, Geochemistry of granitic melts produced during the incongruent melting of muscovite: Implications for the extraction of Himalayan leucogranitic magmas. Jour. Geophys. Res., v. 100, pp. 15767–1577.

Harrison, T. M., McKeegan, K. D., and LeFort, P., 1995, Detection of inherited monazite in the Manaslu leucogranite by $^{208}Pb/^{232}Th$ ion microprobe dating: Crystallization age and tectonic significance. Earth and Planetary Science Letters, v. 133, pp. 271–282.

Harrison, T. M., Ryerson, F. J., LeFort, P., Yin, A., Lovera, O. M., and Catlos, E. J., 1997, A Late Miocene – Pliocene origin for the Central Himalayan inverted metamorphism. Earth and Planetary Science Letters, v. 146, pp. E1–E7.

Harrison, T. M., Grove, M., McKeegan, K. D., Coath, C. D., Lovera, O., and LeFort, P., 1999, Origin and episodic emplacement of the Manaslu Intrusive Complex, Central Himalaya. Jour. Petrology, v. 40, pp. 3–19.

He, D., Webb, A. A., Larson, K. P., Martin, A. J., and Schmitt, A.

K., 2015, Extrusion v duplexing models of Himalayan mountain building 3: duplexing dominates from Oligocene to present. Int. Geol. Rev., v. 57, pp. 1–27.

Hodges, K. V., Parrish, R. R., and Searle, M. P., 1996, Tectonic evolution of the central Annapurna Range, Nepalese Himalaya. Tectonics, v. 15, pp. 1264–1291.

Hopkinson, T., Harris, N., Roberts, N., Warren, C. J., Hammond, S., Spencer, C. J., and Parrish, R. R. 2019, Evolution of the melt source during protracted crustal anatexis: an example from the Bhutan Himalaya. Geology, v.48, pp. 87–91.

Iaccarino, S., Montomoli, C., Carosi, R., Massone, H-J., Langone, A., and Visona, D., 2015, Pressure-temperature-time-deformation path of lyanite-bearing migmatitic paragneiss in the Kali Gandaki alley (Central Nepal): Investigation of Late Eocene-Early Oligocene melting processes. Lithos, v. 231, pp. 103–121.

Jessup, M. J., Law, R. D., Searle, M. P., and Hubbard, M. S., 2006, Structural evolution and vorticity of flowduring extrusion and exhumation of the Greater Himalayan slab, Mount Everest massif, Nepal/Tibet: Implications for orogen-scale flow partitioning. In: Law, R. D., Searle, M. P., and Godin, L. (eds.) Channel Flow, Ductile extrusion and exhumation in continental collision zones. Geol. Soc. London Spec. Pub., v. 268, pp. 379–413.

Jessup, M. J., Cottle, J.M., Searle, M. P., Law, R. D., Newell, D. L., Tracey, R. J., and Waters, D. J., 2009, P-T-t-D paths of Everest series schist, Nepal. Jour. Metam. Geol. doi:10.1111/j.1525-1314.2008.00784x

Kohn, M. J., 2008, P-T-t data from Nepal support critical taper and repudiate large channel flow of the Greater Himalayan Sequence. Geol. Soc. America Bull., v. 120, pp. 259–273.

Larson, K. P. and Cottle, J. M., 2014, Mid-crustal discontinuities and assmebly of the Himalayan mid-crust. Tectonics, v. 33, pp. 718–740.

Larson, K. P., Cottle, J. M., and Godin, L., 2011, Petrochronologyic record of metamorphism and melting in the upper Greater Himalayan sequence, Manaslu-Himalchuli Himalaya, west central Nepal. Lithosphere, v. 3, pp. 379–392.

Law, R. D., Searle, M. P., and Simpson, R. L., 2004, Strain defomration temperatures and vorticity of flow at the top of the Greater Himalayan slab, Everest massif, Tibet. Jour. Geol. Soc. London, v. 161, pp. 305–320.

Law, R. D., Jessup, M. J., Searle, M. P., Francsis, M. K., Waters, D. J., and Cottle, J. M., 2011, Telescoping of isotherms below the South Tibetan detachment, Mount Everest massif. Jour. Struct. Geol., 33, pp. 1569–1594.

LeFort, P., 1975, Himalayas: The collided range. Present knowledge of the continental arc. Am. Jour. Sci., v. 275A, pp. 1–44.

LeFort, P., 1981, Manaslu leucogranite: A collision signature of the Himalaya – a model for its genesis and emplacement. J. Geophys. Res., v. 86, pp. 10545–1068.

LeFort, P., Cuney, C., Deniel, C., France-Lanord, C., Shepard, S., Upreti, B. N., and Vidal, P., 1987, Crustal generation of the Himalayan leucogranites. Tectonophys., v. 34, pp. 39–57.

Martin, J., Ganguly, J., and DeCelles, P. 2010. Metamorphism of greater and lesser Himalayan rocks exposed in the Modi khola valley, central Nepal. Contrib. Min. Pet, v. 159, pp. 203–222.

Montomoli, C., Iaccarino, S., Carosi, R., Longone, A., and Visona, D., 2013, Tectonometamorphic discontinuities within the Greater Himalayan Sequence in western Nepal (Central Himalaya); insights on the exhumation of crystalline rocks. Tectonophys., v. 608, pp. 1349–1370.

Parrish, R. R. and Hodges, K. V., 1996, Isotopic constraints on the age and provenance of the Lesser and Greater Himalayan sequences. Geol. Soc. Am. Bull. v. 108, pp. 904–911.

Parsons, A. J., Law, R. D., Lloyd, G. E., Phillips, R. J., and Searle, M. P., 2016a, Thermo-kinematic evolution of the Annapurna – Dhaulagiri Himalaya, central Nepal: The composite orogenic system. Geochemistry, Geophysics, Geosystems, v. 17, pp. 1511–1539.

Parsons, A. J., Law, R. D., Searle, M. P., Phillips, R. J., and Lloyd, G. E., 2016b, Geology of the Dhaulagiri – Annapurna – Manaslu Himalaya, western region Nepal. Scale 1:200,000. Journal of Maps, v. 12, pp. 100–110.

Parsons, A. J., Phillips, R. J., Lloyd, G. E., Law, R. D., Searle, M. P., and Walshaw, R. D., 2016c, Mid-crustal deformation of the Annapurna – Dhaulagiri Himalaya, central Nepal: an atypical example of channel flow during the Himalayan orogeny. Geosphere, v. 12, pp. 1–31.

Searle, M. P., 1999a, Extensional and compressional faults in the Everest – Lhotse massif, Khumbu Himalaya, Nepal. Jour. Geol. Soc., London, v. 156, pp. 227–240.

Searle, M. P., 1999b, Emplacement of Himalayan leucogranites by magma injection along giant sill complexes: examples from the Cho Oyu, Gyachung Kang and Everest leucogranites (Nepal Himalaya). Jour. Asian Earth Sciences, v. 17, pp. 773–783.

Searle, M. P., 2010, Low-angle normal faults in the compressional Himalayan orogen: Evidence from the Annapurna – Dhaulagiri Himalaya, Nepal. Geosphere, v. 6, pp. 296–315.

Searle, M. P. and Rex, A. J., 1989, Thermal model for the Zanskar Himalaya. Jour. Met. Geol., v. 7, pp. 127–134.

Searle, M. P. and Godin, L., 2003, The South Tibetan Detachment and the Manaslu leucogranite: a structural re-interpretation and reinterpretation of the Annapurna- Manaslu Himalaya. Jour. Geol. v. 11, pp. 505–523.

Searle, M. P. and Szulc, A. G., 2005, Channel Flow and ductile extrusion of the High Himalayan slab, the Kangchenjunga – Darjeeling profile, Sikkim Himalaya. Jour. Asian Earth Sci., v. 25, pp. 173–185.

Searle, M. P., Parrish, R. R., Hodges, K. V., Hurford, A., Ayres, M. W., and Whitehouse, M. J., 1997, Shisha Pangma leucogranite, South Tibetan Himalaya: Field Relations, Geochemistry, Age, Origin and Emplacement. Jour. Geology, v. 105, pp. 295–317.

Searle, M. P., Simpson, R. L., Law, R. D., Parrish, R. R., and Waters, D. J., 2003, The structural geometry, metamorphic and magmatic evolution of the Everest massif, High Himalaya of Nepal – South Tibet. Jour. Geol. Soc. London, v. 160, pp. 344–366.

Searle, M. P., Law, R. D., Godin, L., Larson, K. P., Streule. M. J., Cottle, J. M., and Jessup, M. J., 2008, Defining the Himalayan Main Central Thrust. Jour. Geol. Soc. London, v. 165, pp. 523–534.

Searle, M. P., Cottle, J. M., Streule, M. J., and Waters, D. J., 2010, Crustal melt granites and migmatites along the Himalaya: melt source, segregation, transport and granite emplacement mechanisms. Trans. Royal Soc. Edinburgh: Earth Sciences, v. 100, pp. 219–233.

Shrestha, S., Larson, K. P., Martin, A. J., Guilmette, C., Smit, M. A., and Cottle, J. M., 2020, The Greater Himalayan thrust belt: Insight into the assmebly of the exhumed Himalayan metamorphic core, Modi khola valley, Central Nepal. Tectonics, v. 39, TC006252.

Stephenson, B. J, Searle, M. P., and Waters, D. J., 2001, Structure of the Main Central Thrust zone and extrusion of the High Himalayan crustal wedge, Kishtwar – Zanskar Himalaya. Jour. Geol. Soc. London, v. 158, pp. 637–652.

Streule, M. J., Searle, M. P., Waters, D. J., and Horstwood, M. S. A., 2010, Metamorphism, melting and channel flow in the Greater Himalayan Sequence and Makalu leucogranite: constraints from thermobarometyry, metamorphic modeling and U-Pb geochronology. Tectonics, v. 31, TC5011, pp. 1–28,

Vidal, P., 1978, Rb-Sr systematics in granite from central Nepal (Manaslu); Significance of the Oligocene age and 87Sr/86Sr systematics: Comment, Geology, v. 6, p. 196.

Vidal, P., Cocherie, A., and LeFort, P., 1982, Geochemical investigations of the origin of the Manaslu leucogranite (Himalaya, Nepal). Geochim. et Cosmochim. Acta, v. 46, pp. 2279–2292.

Visona, D., Carosi, R., Montomoli, C., Tiepolo, M., and Peruzzo, L., 2012, Miocene andalusite leucogranite in central-east Himalaya (Everest – Masang Kang area): Low-pressure melting during heating. Lithos, v. 144-145, pp. 194–208.